

SAE AERO DESIGN WEST

“THE WRIGHT STUFF”

By
AARON LOSTUTTER, ADAM NELESSEN, JACOB VINCENT, ZEV
VALLANCE, AND BRANDON PEREZ
Team 10

PROGRESS REPORT

Document

*Submitted towards partial fulfillment of the requirements for
Mechanical Engineering Design – Spring 2013*



Department of Mechanical Engineering
Northern Arizona University
Flagstaff, AZ 86011

Table of Contents

1. Introduction	2
2. Final Concept.....	2
3. Supporting Analysis	3
4. Construction Progress.....	6
5. Finance Review	7
6. Project Timeline	8
7. Appendices	10
7.1. Appendix A	10
7.2. Appendix B	11
7.3. Appendix C	13

List of Tables and Figures

Figure 1: Wing rib.....	2
Figure 2: Cross-section of a hollow shaft for moment of inertia calculation	3
Figure 3: Static thrust test stand.....	4
Figure 4: Plane takeoff schematic.....	5
Figure 5: Wing construction	6
Figure 6: Fuselage construction. Left displays nose side. Right displays tail side.....	7
Figure 7: Gantt chart	9
Table 1: Final dimensions and factors of safety for aluminum spars	3
Table 2: Static thrust testing results	4
Table 3: Important values in takeoff calculations.....	5
Table 4: Financial Overview.....	8

1. Introduction

The following report provides an update on the progress made by “The Wright Stuff” towards the manufacture of a remote-controlled aircraft for participation in the Society of Automotive Engineers (SAE) Aero Design West Competition in April. Since the Final Design Review report, some important developments have been made in this project, centered around the beginning of aircraft construction. This report will give an overview of the final conceptual design, recent supporting analysis, construction progress, project finances, and timeline.

2. Final Concept

As the team began to construct the plane, it became clear that some of our earlier conceptual plans were impractical for this project, given the manufacturing and time constraints. Because of the small scale of the airplane under development, limited time resources, and the material limitations imparted by SAE, the tapered wing planform and the T-tail are very difficult to incorporate into the design. Thus, these were abandoned in favor of the constant chord wing planform and the standard tail, which sits in-plane with the wings. The team will still be pursuing a single high wing configuration, with ribs 3D printed with an ABS polymer. Figure 1 shows one of these ribs.



Figure 1: Wing rib

Spars will be made out of hollow aluminum tubing, which is advantageous for its strength, low cost, and minimal weight. The payload will be secured to the same bolts that connect the wings to the fuselage, with an access bay located underneath the plane. The landing gear will be a tail-dragger configuration, with two wheels mounted to the fuselage base plate and one wheel secured directly underneath the tail.

3. Supporting Analysis

3.1. Spar Design

The process of spar design began with the idealization of a wing as a cantilever beam under uniform distributed loading. Shear force and bending moments were constructed in order to determine critical values of bending stress. Appendix A shows a schematic of this analysis along with the resulting shear force and bending moment diagrams. A base value of 20 lb-ft is used for the dimensioning of the two full-length spars. A middle spar is added, which extends for only the middle 18 inches of the wing, to compensate for any bending moment above that base value. A factor of safety is computed by dividing the material yield strength by the applied bending stress. In this case, the yield strength of the Aluminum 6061 rods is 40 ksi and the applied bending stress is calculated as:

$$\sigma = \frac{Mc}{I} \quad (1)$$

$$\text{where } I = \frac{\pi}{64}(D^4 - d^4) \quad (2)$$

Figure 2 shows these D and d values on a hollow shaft.



Figure 2: Cross-section of a hollow shaft for moment of inertia calculation

Table 1 displays the results of this analysis, including outer and inner diameters and the minimum factor of safeties for each spar. Note that the minimum factor of safety of near 1.5 is a common value for unmanned aerial vehicles such as these.

Table 1: Final dimensions and factors of safety for aluminum spars

Spar	Front	Rear	Middle
Length (ft)	7	7	1.5
OD (in)	1/2	3/8	5/8
ID (in)	0.402	0.305	0.509
Min FS	1.79	1.46	3.73

Appendix B provides the code that was used to perform this analysis.

3.2. Static Thrust Testing

The group performed static thrust testing in order to determine the propeller that would provide the maximum amount of thrust to the aircraft. For this experiment, a test stand was constructed in order to directly determine the force produced by the engine. The static thrust test stand is shown in Figure 3.



Figure 3: Static thrust test stand

This task was performed in Phoenix, Arizona because the air density there is close to that of the competition location. During the testing of four different propellers, the maximum thrust values and corresponding rotation per minute values were recorded.

Following this experiment, the selected propeller is a 13x4 propeller. While the 14x4 propeller did produce more thrust than the 13x4, it imparted an excessive amount of strain on the engine. Therefore, the group selected the 13x4 propeller for its final choice. The results of this experiment are shown in Table 2.

Table 2: Static thrust testing results

Prop Size	RPM	Thrust (N)
11X7	11,400	24.5
12X7	10,000	23.2
13X4	10,500	32.4
14X4	9,300	36.3

3.3. Takeoff Calculations

Following the static thrust testing, the team was able to develop a modeling tool to predict the distance that will be required for the airplane to achieve takeoff. This involves the use of MATLAB to solve a one-dimensional dynamics problem, which is made possible by

assuming that the plane will experience constant acceleration. This assumption is realistic, since the plane will be held until the engine achieves the maximum rotation rate at the competition. A schematic for this solution is shown in Figure 4.



Figure 4: Plane takeoff schematic

The equations for the solution of this problem are:

$$V^2 = V_0^2 + 2a(x - x_0) \quad (3)$$

$$x = V^2/2a \quad (4)$$

Inputs to this MATLAB code are the weight of the plane, static thrust, and the velocity at which the appropriate amount of lift will be provided to pick the plane up off the ground. The result of this program is an output of the distance required. At this stage in the design process, this code is useful for giving the team a reference point for the maximum weight allowable if the plane is to take off within the required distance of 200ft. Once the plane construction is complete, the final weight will be included in this calculation to determine the actual takeoff distance. Table 3 shows the first iteration of this calculation. Appendix C below includes the code used to conduct this analysis.

Table 3: Important values in takeoff calculations

Summary of Takeoff Characteristics		
Static Thrust	(lb)	7
	(N)	32
Plane Weight	(lb)	40
	(N)	18
Plane Acceleration	(ft/s ²)	6
	(m/s ²)	2
Desired Velocity	(ft/s)	48
	(m/s)	15
Distance	(ft)	194
	(m)	59

4. Construction Progress

4.1. Wings

Wing construction was approached from two directions, conventional techniques, and 3D printing and assembly. Considering conventional methods first, the core of the wing is built around a solid wing section which rests on top of the fuselage.

This ‘interior’ wing section is constructed from layered medium density balsa has been constructed to, when mounted, precisely match wing rib profiles at the desired 6° angle of attack. Lengthwise holes through the wing core allow exact fitting of the three spars which run along the length of the wing.

Along the length of the 6’ spars, ribs have been fitted every three inches. To improve torsional stiffness along the wing length, the leading edges of the front section of the ribs will be covered with a thin layer of heat-treated balsa, while on the rear rib sections a single balsa beam will be fitted to strengthen aileron edges.

Figure 5 displays the wing in its current state, including the solid wing section, three hollow aluminum spars, and ABS polymer ribs.



Figure 5: Wing construction

4.2. Fuselage

Constructing an adequate fuselage is an effort in balancing material usage and structural rigidity. For a heavy lift application, it is imperative that the plane be built in such a way that being loaded significantly doesn't affect the mechanical and structural performance of the aircraft.

To achieve this high-load rigidity, a lightweight aluminum honeycomb panel was cut as seen in Figure 6, to provide a backbone for the entire air structure. This honeycomb panel has been drilled with three holes through which bolts can be run to secure the wing to the fuselage, and the payload to the interior of the aircraft.

Directly attached to this panel and running about four feet to the tail, are two sets of custom balsa angle beams, providing a high level of flexural stiffness from nose to tail of the craft, while minimizing the amount of construction material needed. Held between the four stringers are five basswood bulkheads, adding torsional stiffness to the aircraft as well as mounting locations for the engine and electronics. Figure 6 shows a view from tail to nose, displaying bulkheads and balsa stringers.

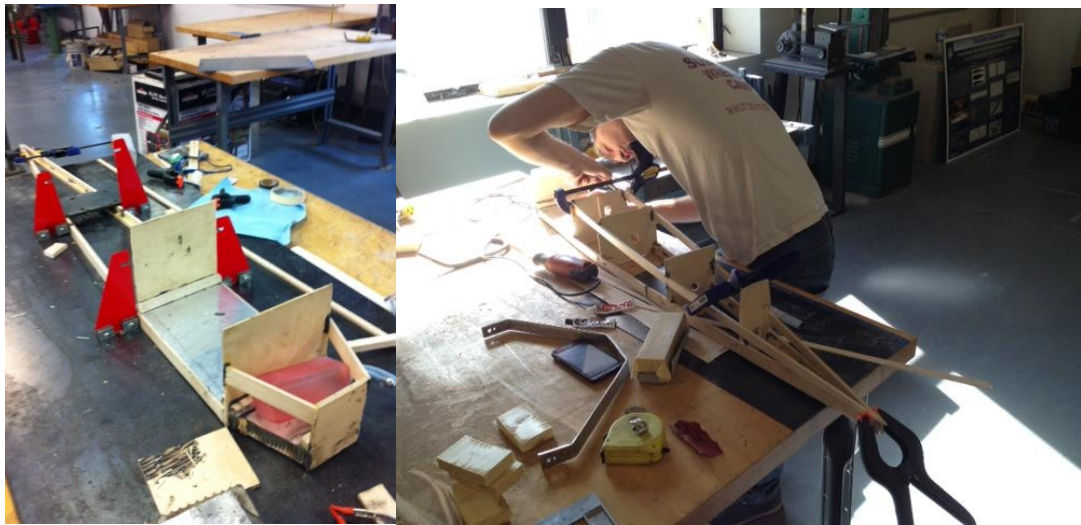


Figure 6: Fuselage construction. Left displays nose side. Right displays tail side.

5. Finance Review

Table 4 shows the state of team finances as of the date of submission of this report. The team has raised \$5000 dollars in support of this project, which fully covers the anticipated costs as outlined in previous reports. The team has already made most of the anticipated purchases, including core materials, hotel reservations, building supplies, and the competition registration. Despite these purchases, a surplus of funds remains. Most likely, these additional funds will be used to make repairs or adjustments after the first flight test and to build alternative components like wings or tails.

Table 4: Financial Overview

Building Budget	\$1,835
Travel Budget	\$2,250
Competition Budget	\$870
Total Budget	\$5,000
Expenses	\$2,762
Remaining Budget	\$2,238

6. Project Timeline

Figure 7 shows the Gantt chart, current as of the submission of this report. This chart is color-coded to differentiate between the different types of tasks being completed by the team. The blue items are related to construction of the airplane, the red refer to fulfillment of SAE requirements, and the green show requirements for the Capstone class. Currently, the group is in the midst of the Prototype 1 Construction phase. The nearest major deadline is the submission of the SAE report, due March 4, which must include all details of the design that will be flown in the competition in April.

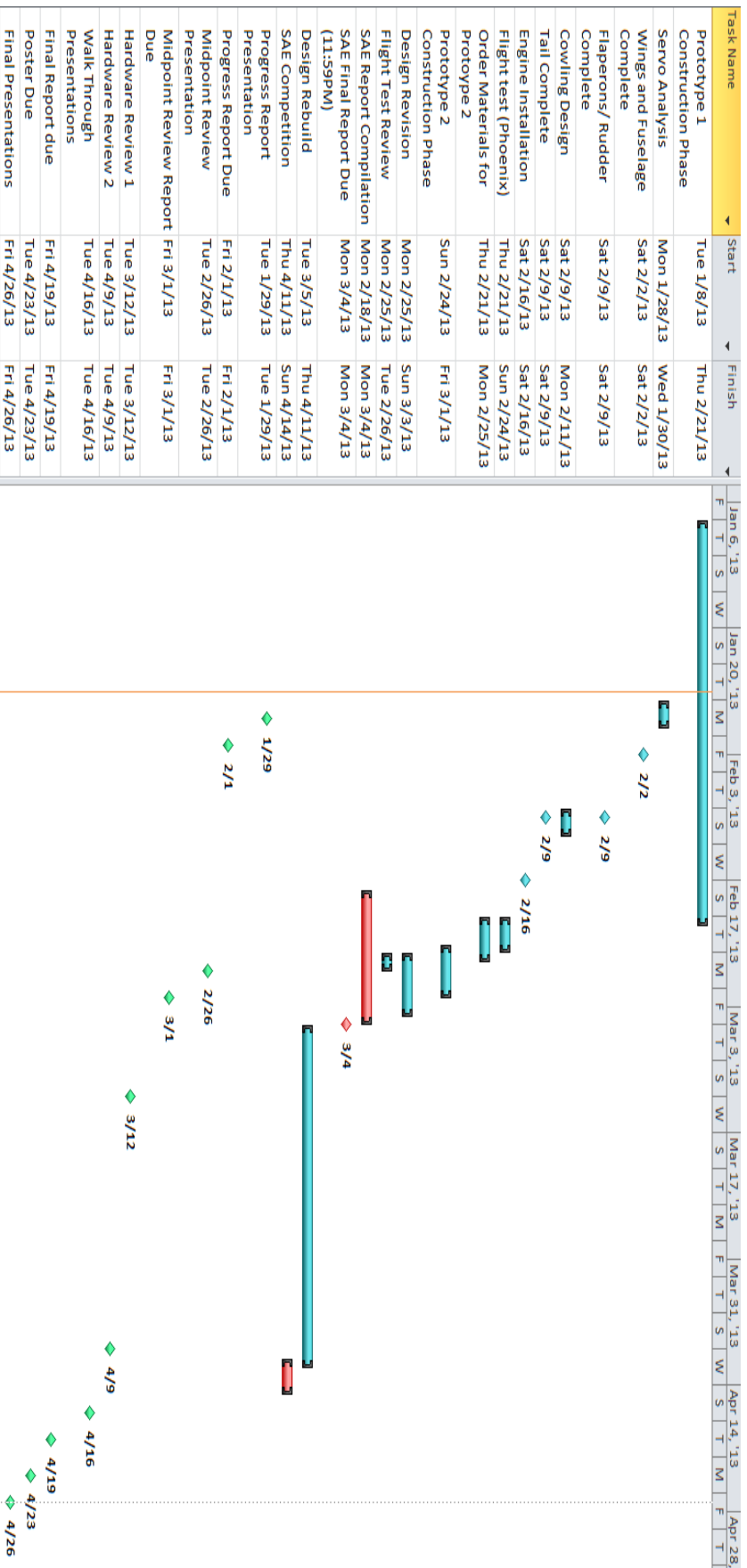
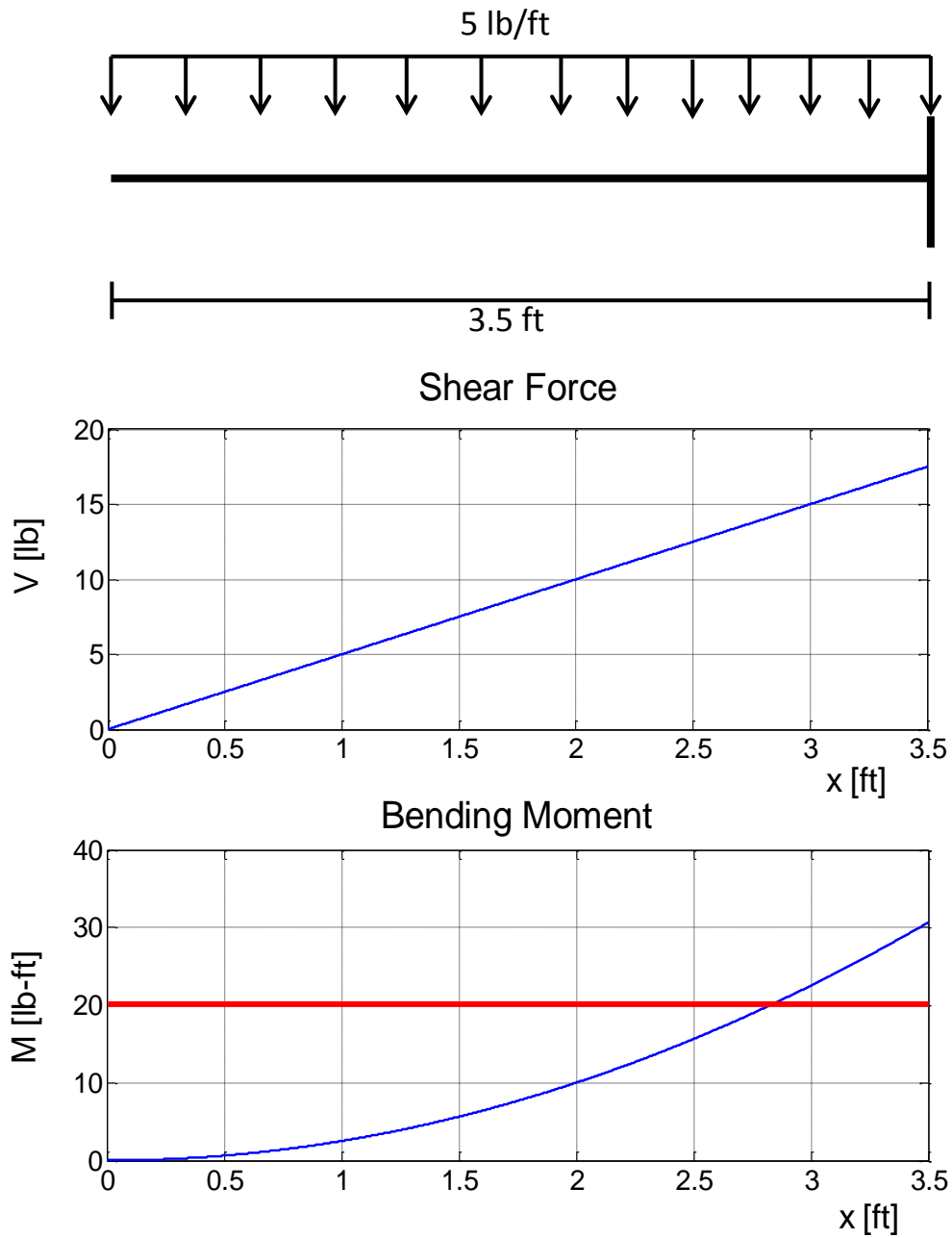


Figure 7: Gantt chart

7. Appendices

7.1. Appendix A



7.2. Appendix B

```
%% Cleanup
clear all; clc; close all;

%% Input wing length and max/min applied loads
L=3.5;
W1=5;
Total_Lift=2*L*W1;
%% Resolve distributed load into point loads
F1=W1*L;

%% Reactions at front spar support
By=F1;
Mb=L/2*F1;

%% Equations for Shear Force and Bending Moment
x=0:.001:L;
for i=1:length(x)
    V(i)=x(i)*W1;
    M(i)=x(i)^2*W1/2;
end

%% V&M Diagrams
subplot(2,1,1)
plot(x,V)
xlabel('x [ft]')
ylabel('V [lb]')
title('Shear Force')
grid on

subplot(2,1,2)
plot(x,M);
xlabel('x [ft]')
ylabel('M [lb-ft]')
title('Bending Moment')
grid on

Mmax=max(M);      %ft-lb
Vmax=max(V);      %ft-lb
Mmax_in=Mmax*12;%lb-in
Mmed=20*12;       %lb-in

%% Strength Calculations for Front Spar - Cyl
yield=40;         %metalsdepot.com & mcmaster

t1_cyl=.049;
do1=1/2;
Io1=(pi/64)*do1^4; %in^4

di1=do1-2*t1_cyl;
Ii1=(pi/64)*di1^4; %in^4

Iloverall=Io1-Ii1;
```

```

y1_cyl=do1/2;    %in

FS_front_cyl=yield/(((2/3)*Mmed*y1_cyl)/I1overall)/1000) %ksi

A1cyl=(pi/4)*(do1^2-di1^2);
V1cyl=6*12*A1cyl;

%% Strength Calculations for Rear Spar - Cyl
yield=40;        %metalsdepot.com

t2_cyl=.035;
do2=3/8;
Io2=(pi/64)*do2^4;    %in^4

di2=do2-2*t2_cyl;
Ii2=(pi/64)*di2^4;    %in^4

I2overall=Io2-Ii2;

y2_cyl=do2/2;    %in

FS_rear_cyl=yield/(((1/3)*Mmed*y2_cyl)/I2overall)/1000) %ksi

A2cyl=(pi/4)*(do2^2-di2^2);
V2cyl=6*12*A2cyl;

%% Middle Spar - Cyl
t3_cyl=.058;
do3=5/8;
Io3=(pi/64)*do3^4;%in^4

di3=do3-2*t3_cyl;
Ii3=(pi/64)*di3^4;
y3=do3/2;    %in

I3overall=Io3-Ii3;

FS_mid_cyl=yield/(((.6*Mmed*y3)/I3overall)/1000) %ksi

A3cyl=(pi/4)*do3^2;
V3cyl=1.5*12*A3cyl;

Wt=(V1cyl+V2cyl+V3cyl)*0.0975

```

7.3. Appendix C

```

clc; clear all;

weight=40;           %lb
speed_particular=32.50*.447; % [m/s]

thrust=3.3*9.81;     %N
thrust_ib=thrust*.22481; %ib
mass=weight*.4536;  %kg
accel=thrust/mass;  %m/s^2
accel_ft=accel/.3048; %ft/s^2
speed_particular_ft=speed_particular/.3048;
distance=speed_particular^2/(2*accel);
distanceft=distance/.3048;

T=283.15;           % [K] from wunderground avg on 4/14
p=98532.6;          % [Pa] from wunderground avg on 4/14
R=287.04;           % [J/kg*K] Air
rho=p/(R*T);        % [kg/m^3]
qinf_particular=.5*rho*speed_particular^2; % [N/m^2]
chordft=1;%input('\nInput Chord at the root in ft: \n');
chord=chordft*.3048;
cl=1.845;%input('\nInput cl from XFOIL: \n');
Lprime=cl*qinf_particular*chord/4.448; % [lb/m]
Lwings=Lprime*6.5*.3048; %lb
Ltotal=1.25*Lwings;

fprintf('                Summary of Takeoff
Characteristics                \n');
fprintf('\n');
fprintf('                |   Static Thrust   |   Plane Weight   |   Plane
Acceleration | Desired Velocity |   Distance   |\n');
fprintf('                |---[lb]---|---[N]---|---[lb]---|---[N]---|---[ft/s^2]---|---
[m/s^2]---|---[ft/s]---|---[m/s]---|---[ft]---|---[m]---|\n');
fprintf('                |   %.1f   |   %.1f   |   %.1f   |   %.1f   |   %.1f   |
%.1f   |   %.1f   |   %.1f   |   %.1f   |   %.1f   |
|\n',thrust_ib,thrust,weight,mass, accel_ft, accel, speed_particular_ft,
speed_particular, distanceft, distance);

```